doi:10.2533/chimia.2025.255 Chimia 79 (2025) 255–258

Determination of the Absolute Configuration by 3D ED to Elucidate the Atroposelectivity in Aromatic Ring-Opening Metathesis

Valeriia Hutskalova[§a*], Christian Jandl[b], Alessandro Prescimone[c], and Christof Sparr[a]

[§]SCS-dsm-firmenich Award for the best poster presentation in Organic Chemistry

Abstract: The determination of the absolute configuration of molecules bearing different stereogenic elements represents a fundamental and indispensable task in the field of stereochemistry. Whereas X-ray crystallographic analysis has been established as a broadly utilized and reliable technique to achieve this goal, limitations remain arising from the demanding requirements for the size and diffraction quality of the analyzed crystals. As an emerging technique, 3D microcrystal electron diffraction (3D ED) has increasingly been recognized to complement single crystal X-ray diffraction (SC-XRD). Having encountered challenges in determining the absolute configuration for the products obtained during the development of atroposelective aromatic ring-opening metathesis (AArROM), we herein describe in detail, how 3D ED allowed an assignment, which proved unfeasible using the conventional approach with X-ray crystallography.

Keywords: 3D ED · Absolute configuration · Atropisomerism · Metathesis

Valeriia Hutskalova received her BSc in Chemistry from Taras Shevchenko National University of Kyiv in 2019. During her studies, she also worked as a synthetic chemist and later as an assistant project manager at Enamine Ltd. Valeriia then joined the Sparr group as an Alfred Werner scholar for her Master's studies to develop new synthetic methods for the preparation and application of acridinium photocatalysts. In 2020, she started her PhD studies with a focus on the development of novel photoredox- and transition metal-catalyzed (atroposelective) synthetic methods, including aromatic ring-opening metathesis.

1. Introduction: Aromatic Ring-Opening Metathesis (ArROM)

Being among the few reactions recognized with a Nobel Prize, alkene metathesis catalyzed by transition metal alkylidenes has emerged as one of the most powerful and reliable approaches for carbon–carbon bond-forming and -breaking transformations.[1–3] For non-aromatic structures, substantial advancements have been achieved over the past decades, as evidenced by the development of efficient catalysts and the immense repertoire of cross-, ring-opening, and ring-closing metathesis reactions (CM, ROM, and RCM), including the implementation of metathesis in total synthesis of complex natural products.[4] In stark contrast to the well-explored alkene and alkyne metathesis, metathesis to promote the opening of arenes has remained elusive and rather counterintuitive. According to reported density functional theory calculations of metathesis reactions of a selected range of benzene derivatives,[5] it was concluded that benzene represents an infeasible substrate for ring-opening metathesis due to the highly unfavorable energetics caused by the loss of aromaticity upon generation of the crucial Ru metallacyclobutane intermediate. To evaluate this paradigm that aromatic rings cannot be cleaved by ring-opening metathesis, we recently studied aromatic ring-opening metathesis (ArROM)[6] driven by the formation of stabilized aromatic ring systems and strain release (Scheme 1a). The approach to directly cleave arenes in a catalytic fashion proved to be highly efficient for both six- and five-membered aromatic systems, and the viability and generality of ArROM were demonstrated across a wide array of substrates (Scheme 1a). With the new opportunities unveiled by the ArROM reactions, we investigated whether control over the configuration of stereogenic axes could be achieved. In these studies, the viability of atroposelective ArROM (AArROM) was confirmed by the highly stereoselective synthesis of C–C and C–N atropisomers using chiral Schrock–Hoveyda[7] molybdenum catalysts (Scheme 1b). Having investigated the generality of the developed strategies by a substrate scope exploration, we moved to the next crucial step: the determination of the absolute configuration of the obtained products.

2. Absolute Configuration Determination

2.1 *X-Ray Crystallography*

To elucidate the absolute configuration of biphenanthrenes obtained through the combination of atroposelective ArROM with twofold RCM, single crystals of product **1** (Scheme 1b) for SC-XRD were obtained by solvent layering of dichloromethane and methanol. With a suitable Flack parameter (x = 0.04(7)), the absolute configuration was assigned to (S_a)-**1**. However, during the investigation of synthesized C–N atropisomers, we encountered that numerous attempts to grow a suitable enantiopure crystal for SC-XRD of the phenanthrenyl-indole product **2** did not give a sample of high diffraction quality (Scheme 1b). Specifically, no data could be collected upon mounting the obtained crystals of **2**

*Correspondence: V. Hutskalova, E-mail: valeriia.hutskalova@unibas.ch.
[a]Department of Chemistry, University of Basel, St. Johanns-Ring 19, CH-4056 Basel, Switzerland; [b]ELDICO Scientific AG, Switzerland Innovation Park Basel Area, Hegenheimermattweg 167 A, CH-4123 Allschwil, Switzerland; [c]Department of Chemistry, University of Basel, BPR 1096, Mattenstrasse 24a, CH-4058 Basel, Switzerland

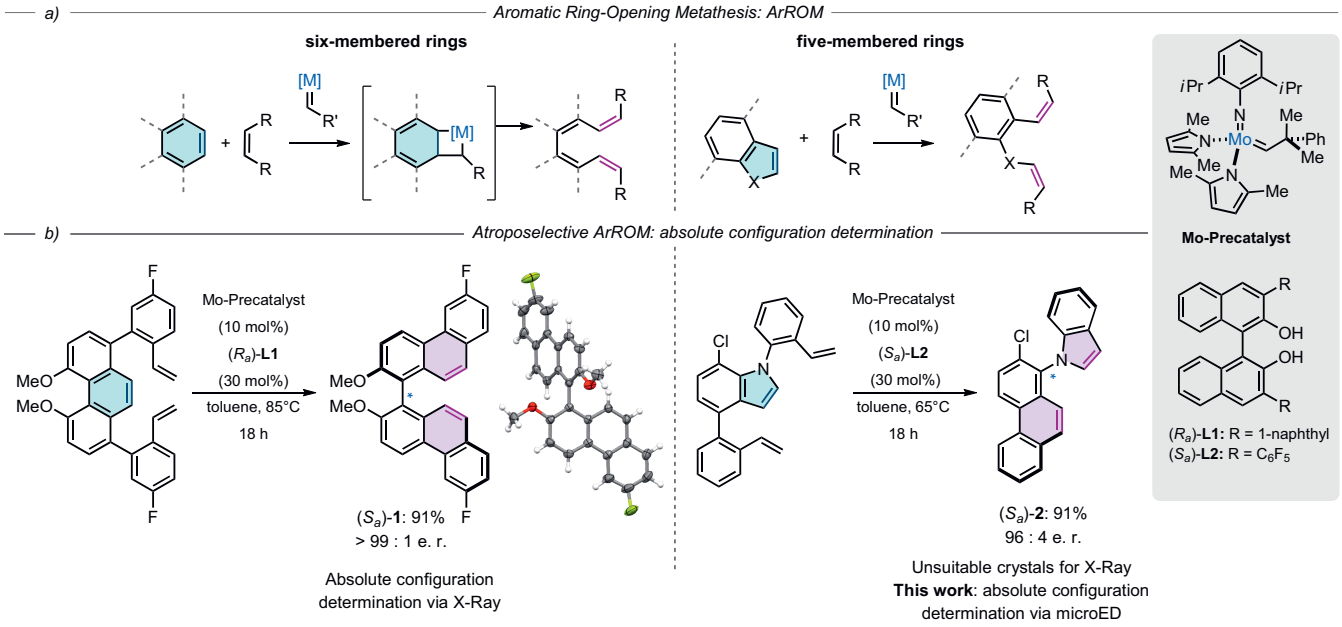

Scheme 1. a) Overview of the recently developed aromatic ring-opening metathesis (ArROM) of six- and five-membered ring systems; b) Determination of the absolute configuration of the obtained enantioenriched products.

with a standard microfocussed Cu source at 150 K due to their weak diffraction. Owing to the small size of the crystals, which approached the limit for SC-XRD (around 10 µm), several data collections were also attempted at 150 K on a different diffractometer equipped with a metaljet Ga source in combination with long exposures to maximize the chances of success. Unfortunately, the crystals proved to be prone to radiation damage as the high intensity of the metaljet source rapidly (within 1–2 hours) damaged every crystal that was subjected to the measurements, well before any usable data could be collected. The small size and fragility of crystals of compound **2** rendered SC-XRD unsuitable for the absolute configuration determination. Furthermore preparation of quasi-racemic mixtures[8] also did not lead to the formation of crystals suitable for X-ray crystallography. With the emerging capabilities of microcrystal electron diffraction (3D ED) and its advantages, particularly the ability to utilize crystals much smaller than those required for SC-XRD, we opted to explore this technique to assign the absolute configuration of **2**.

2.2 *Electron Diffraction (ED): General Overview*

3D electron diffraction (3D ED), also called microcrystal electron diffraction (microED) or simply electron diffraction (ED), has seen a very fast development in recent years and can now be considered a routine tool for crystal structure determination.[9–12] Whereas in the past the only way to perform 3D ED experiments involved modifying a transmission electron microscope (TEM), there are now both electron microscopes with built-in ED functionalities and turn-key electron diffractometers on the market. The service has become available through commercial providers, research institutes, and national facilities.[13,14] 3D ED can be employed as an alternative when conventional structure elucidation *via* SC-XRD fails due to insufficient crystal size, because the stronger interaction of electrons with matter as compared to X-rays makes it possible to collect 3D diffraction data from crystallites far below 1 µm in thickness – out of reach not only for any in-house X-ray sources, but also for synchrotrons.[10,12] While 1 µm is often defined as the upper size limit for ED, our experience suggests a thickness of up to 2–3 µm to be still feasible for light atom structures like typical organic molecules, even though data quality is reduced.[13] For practical purposes this upper size limit is not an obstacle as 1) crystal size can be readily reduced by grinding (compounds sensitive to mechanical stress are a rare exception) and 2) even for larger crystals it is often possible to collect data by pointing a nanobeam at an edge or corner, where they are thinner. A lower size limit of *ca*. 50 nm has been estimated for ED, which is connected to the number of consecutive unit cells required for good diffraction quality and is therefore highly dependent on the specific sample.[15] The suitable size range for ED thus covers what is considered a powder by X-ray diffraction standards. However, compared to powder X-ray diffraction (PXRD), structure determination with ED is much easier and more universal as it can be used even for very complex molecules up to proteins, but PXRD is still valuable as a complimentary technique to check the bulk representativity of structures determined with ED.[15] Further advantages of 3D ED include the ability to work with very small amounts of substances and with phase mixtures.[10]

Currently, the classical use case for 3D ED are for compounds where SC-XRD has failed; however, integrating ED earlier in the workflow holds huge potential to speed up research. Being able to use crude powder material without the need for crystal growth or even purification has proven to be essential in several recent studies.[14,16–20] As mentioned, the stronger interaction of electrons with matter is why ED can work with crystals orders of magnitude smaller than SC-XRD, but this also comes at a cost. One of the consequences is beam damage, which is particularly relevant for organic compounds, and even though strategies like measuring at low temperatures and with low beam intensity exist, they can only reduce and not prevent the degradation of sensitive materials in the electron beam.[10,12] The radiation sensitivity is highly sample dependent: with typical measurement times of 1–2 minutes on state-of-the-art instruments, some compounds can be measured at room temperature without significant degradation, whereas others completely lose crystallinity within seconds under the same conditions. To estimate the sensitivity of a given molecule, one can follow some empiric rules stating that aromatic groups and hydrogen bonding increase beam stability, whereas (especially long) aliphatic chains and reduction-sensitive groups lead to the opposite effect. Another consequence of the strong interaction of electrons with matter is the occurrence of multiple scattering events within the crystal, also known as dynamical effects, whereas for X-ray diffraction the kinematical approximation (*i.e.* assuming only single scattering) is sufficient.[10,12] This affects the reflection intensi-

ties, effectively making them 'worse' as long as data are treated within the kinematical approximation, and therefore constitutes the main reason why structure models from ED are in general of lower quality than those from SC-XRD.[10,21] Lower quality, of course, does not imply that the structures are incorrect: in cases where a compound was analyzed both by 3D ED and SC-XRD, the same structure was obtained, only the molecular geometries and displacement parameters from ED were less accurate.[21–27] The structure models can be improved by employing the dynamical theory of diffraction for refinement, which yields better molecular geometries and gives insights into structural details like occupancies and hydrogen positions.[10,21] Concerning the latter, ED also has an advantage over SC-XRD as the scattering factors make it more sensitive to light atoms, but in most cases, this will only show up if dynamical refinement is performed, because otherwise, the dynamical effects create too much noise in the data.[10,21,28,29] The reason why dynamical refinement is not used on a routine basis can be found in the computational effort, which makes it very time consuming.[10,23] Potentially the biggest benefit of dynamical refinement is the ability to determine absolute structures as the interference of multiple beams makes the reflection intensities very sensitive to the enantiomorph without the need for heavy atoms to be present.[10,21,30] The method is very robust and has been successfully employed in a growing number of publications,[13,21,25,29–36] including (S_a)-1-(2-chlorophenanthren-1-yl)-1*H*-indole (**2**) from our recent publication.[6]

2.3 *ED: Detailed Procedure for (S_a)-2*

Following the unsuccessful attempts to grow sufficiently large crystals of **2** for SC-XRD, a clump of needles was taken from the mother liquor of the crystallization batch, left to dry in air, and then ground gently between two microscope slides. The dry powder was deposited on a standard TEM grid (amorphous carbon on copper) and measured on an ELDICO *ED-1* electron diffractometer using the software ELDIX.[37] The device is equipped with a LaB_6 electron source operating at an acceleration voltage of 160 kV (λ = 0.02851 Å) and a hybrid-pixel detector (Dectris QUADRO). The grid was screened for suitable crystals in the STEM (scanning transmission electron microscopy) mode and after taking a single diffraction frame to assess the crystal quality, diffraction data were collected in the continuous rotation mode with a beam of *ca*. 750 nm diameter. 15 particles were measured and the best four were selected for solution and refinement (see Table 1). Parts of the measurements affected by beam damage or shadowing by the grid were omitted. For kinematical refinement, data were processed with the Apex4 software package.[38] Frames were integrated separately, then merged, scaled, and corrected for Lorentz effects, scan speed, background, and absorption using SAINT and SADABS.[39,40] Space group determination was based on systematic absences, E statistics, and successful refinement of the structure. The structure was solved using ShelXD and refined with ShelXL in conjunction with ShelXle.[41–43]

Least squares refinements were carried out within the kinematic approximation by minimizing $\Sigma w(F_{obs}^2-F_{calc}^2)^2$ with the ShelXL weighting scheme and using neutral electron scattering factors.[42,44] An extinction correction was used as an empirical approach to partly account for the effects of dynamical diffraction. Non-H atoms were refined with anisotropic displacement parameters and no restraints were used in the refinement. H atoms were placed in calculated positions based on typical distances for neutron diffraction and refined with a riding model and $U_{iso}(H) = 1.2 \cdot U_{eq}(C)$. The structure obtained this way was used as a structure model for dynamical refinement (see Fig. 1).

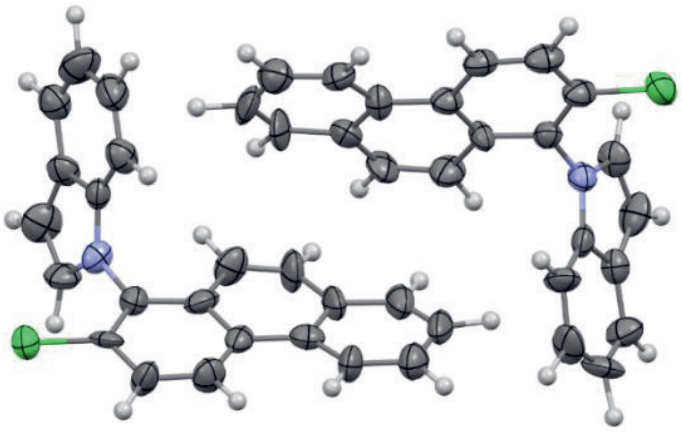

Fig. 1. Asymmetric unit of the crystal structure of (S_a)-**2** with two independent molecules.

For dynamical refinement, data were processed using the PETS2 software package.[45] Unit cells were re-determined and the frames were integrated, corrected for pattern orientation and beam position, and merged into overlapping virtual frames of 3° per frame with a distance between frames of 2°.[28] Dynamical refinement was performed based on least squares refinement of $\Sigma w(I_{obs}-I_{calc})^2$ using the JANA2020 software package and assuming uniform thickness of the crystals.[46] The structure model from kinematical refinement was kept fixed and only parameters specific to the dynamical approach were refined. Such a 'reduced' dynamical refinement does not give improvements of the structure model but saves a lot of computing time and is sufficient for reliable absolute structure determination.[13,21,36] The dynamical refinement results for 4 individual crystals of (S_a)-**2** are shown in Table 2. Both enantiomorphs were refined for each crystal and the R factors consistently show a much better fit for the S_a form. As an additional validation, the *z*-score was used, which is a statistical measure of the significance of the result; a *z*-score >3σ is usually considered as reliable.[21] With all values above 10σ and one

Table 1. Continuous rotation 3D ED data collection details for (S_a)-**2**, ϕ represents the rotation angle, $\Delta\phi$ and Δt are the rotation and exposure per frame.

Crystal	ϕ range [°]	$\Delta\phi$ [°]	Δt [s]	Frames measured	Frames used
1	–60 to 30	1	1	90	41–90
2	–70 to 40	1	1	110	1–100
3	–65 to 65	1	1	130	11–120
4	–60 to 60	1	1	120	1–110

Table 2. Dynamical refinement results for both enantiomorphs of (S_a)-**2**.

	(R_a)-enantiomorph		(S_a)-enantiomorph		
Crystal	R_1(obs)	ωR_2(all)	R_1(obs)	wR_2(all)	*z*-score
1	16.16	30.28	13.10	25.46	10.34
2	18.54	36.53	14.89	29.86	12.48
3	19.03	34.85	16.12	30.23	11.89
4	16.86	32.78	11.48	22.47	22.03

crystal even above 20σ the confidence level in the determination of the S_a enantiomer is outstanding.

3. Conclusions

In summary, we have illustrated the benefits of 3D ED in determining the absolute configuration, showcased by an atropisomer bearing a stereogenic C–N axis, where conventional SC-XRD proved unfeasible. Overall, it is anticipated that due to the immense developments in 3D ED, it will soon be routinely integrated in synthetic chemistry as a complementary approach to SC-XRD.

Acknowledgements

V. H. wants to thank the Swiss Chemical Society and dsm-firmenich for the best poster presentation award. This project has received funding from the European Research Council (ERC) under the European Union's Horizon 2020 research and innovation programme (grant agreement number 101002471), the Swiss National Science Foundation (10001653) and the Swiss Nanoscience Institute (microED).

Received: February 28, 2025

[1] A. Fürstner, *Angew. Chem. Int. Ed.* **2000**, *39*, 3012, https://doi.org/10.1002/1521-3773(20000901)39:17<3012::AID-ANIE3012>3.0.CO;2-GÜ.
[2] O. M. Ogba, N. C. Warner, D. J. O'Leary, R. H. Grubbs, *Chem. Soc. Rev.* **2018**, *47*, 4510, https://doi.org/10.1039/C8CS00027A.
[3] Z. Joncev, C. Sparr, *Angew. Chem. Int. Ed.* **2022**, *61*, e202211168, https://doi.org/10.1002/anie.202211168.
[4] I. Cheng-Sánchez, F. Sarabia, *Synthesis* **2018**, *19*, 3749, https://doi.org/10.1055/s-0037-1610206.
[5] A. Poater, M. C. D'Alterio, G. Talarico, R. Chauvin, *Eur. J. Org. Chem.* **2020**, *2020*, 4743, https://doi.org/10.1002/ejoc.202000725.
[6] V. Hutskalova, C. Sparr, *Nature* **2025**, *638*, 697, https://doi.org/10.1038/s41586-024-08472-z.
[7] J. B. Alexander, D. S. La, D. R. Cefalo, A. H. Hoveyda, R. R. Schrock, *J. Am. Chem. Soc.* **1998**, *120*, 4041, https://doi.org/10.1021/ja974353i.
[8] X. Wu, J. Malinčík, A. Prescimone, C. Sparr, *Helv. Chim. Acta* **2022**, *105*, e20220011, https://doi.org/10.1002/hlca.202200117.
[9] C. G. Jones, M. W. Martynowycz, J. Hattne, T. J. Fulton, B. M. Stoltz, J. A. Rodriguez, H. M. Nelson, T. Gonen, *ACS Cent. Sci.* **2018**, *4*, 1587, https://doi.org/10.1021/acscentsci.8b00760.
[10] M. Gemmi, E. Mugnaioli, T. E. Gorelik, U. Kolb, L. Palatinus, P. Boullay, S. Hovmöller, J. P. Abrahams, *ACS Cent. Sci.* **2019**, *5*, 1315, https://doi.org/10.1021/acscentsci.9b00394.
[11] T. Gruene, J. J. Holstein, G. H. Clever, B. Keppler, *Nat. Rev. Chem.* **2021**, *5*, 660, https://doi.org/10.1038/s41557-023-01186-1.
[12] A. Saha, S. S. Nia, J. A. Rodríguez, *Chem. Rev.* **2022**, *122*, 13883, https://doi.org/10.1021/acs.chemrev.1c00879.
[13] P. Simoncic, E. Romeijn, E. Hovestreydt, G. Steinfeld, G. Santiso-Quiñones, J. Merkelbach, *Acta Crystallogr., Sect. E:Crystallogr. Commun.* **2023**, *79*, 410, https://doi.org/10.1107/S2056989023003109.
[14] M. Aragon, S. E. J. Bowman, C.-H. Chen, M. J. de la Cruz, D. A. Decato, E. T. Eng, K. M. Flatt, S. Gulati, Y. Li, C. J. Lomba, B. Mercado, J. Miller, L. Palatinus, W. J. Rice, D. Waterman, C. M. Zimanyi, *Acta Crystallogr., Sect. C:Struct. Chem.* **2024**, *80*, 179, https://doi.org/10.1107/S2053229624004078.
[15] Y. Yun, X. Zou, S. Hovmöller, W. Wan, *IUCrJ* **2015**, *2*, 267, https://doi.org/10.1107/S2052252514028188.
[16] A. Wagner, J. Merkelbach, L. Samperisi, N. Pinsk, B. M. Kariuki, C. E. Hughes, K. D. M. Harris, B. A. Palmer, *Cryst. Growth Des.* **2024**, *24*, 899, https://doi.org/10.1021/acs.cgd.3c01290.
[17] D. Trzybiński, M. Ziemniak, B. Olech, S. Sutuła, T. Góral, O. Bemowska-Kałabun, K. Brzost, M. Wierzbicka, K. Woźniak, *Molecules* **2024**, *29*, 4916, https://doi.org/10.3390/molecules29204916.
[18] E. Danelius, G. Bu, L. H. E. Wieske, T. Gonen, *ACS Chem. Biol.* **2023**, *18*, 2582, https://doi.org/10.1021/acscentsci.3c01365.
[19] T. Sasaki, T. Nakane, A. Kawamoto, T. Nishizawa, G. Kurisu, *CrystEngComm* **2023**, *25*, 352, https://doi.org/10.1039/D2CE01522F.
[20] D. Marchetti, A. Pedrini, C. Massera, M. D. Faye Diouf, C. Jandl, G. Steinfeld, M. Gemmi, *Acta Crystallogr., Sect. B:Struct. Sci., Cryst. Eng. Mater.* **2023**, *79*, 432, https://doi.org/10.1107/S2052520623007680.
[21] P. B. Klar, Y. Krysiak, H. Xu, G. Steciuk, J. Cho, X. Zou, L. Palatinus, *Nat. Chem.* **2023**, *15*, 848, https://doi.org/10.1038/s41557-023-01186-1.
[22] L. R. Doyle, E. A. Thompson, A. L. Burnage, A. C. Whitwood, H. T. Jenkins, S. A. Macgregor, A. S. Weller, *Dalton Trans.* **2022**, *51*, 3661, https://doi.org/10.1039/D2DT00335J.
[23] L. S. de Moraes, J. E. Burch, D. A. Delgadillo, I. H. Rodriguez, H. Mai, A. G. Smith, S. Caille, S. D. Walker, R. P. Wurz, V. J. Cee, J. A. Rodriguez, D. Gostovic, K. Quasdorf, H. M. Nelson, *Org. Lett.* **2024**, *26*, 6944, https://doi.org/10.1021/acs.orglett.4c01865.
[24] B. Wang, J. F. Bruhn, A. Weldeab, T. S. Wilson, P. T. McGilvray, M. Mashore, Q. Song, G. Scapin, Y. Lin, *Chem. Commun.* **2022**, *58*, 4711, https://doi.org/10.1039/D2CC00221C.
[25] D. Decato, L. Palatinus, A. Stierle, D. Stierle, *Acta Crystallogr., Sect. C:Struct. Chem.* **2024**, *80*, 143, https://doi.org/10.1107/S2053229624003061.
[26] D. T. Ungur, A. Lanza, D. Stam, C. Guguta, C. Iordache, V. Fruth, G. Santiso-Quinones, M. M. Pop, *CrystEngComm* **2024**, *26*, 4295, https://doi.org/10.1039/D4CE00518J.
[27] J. F. Bruhn, G. Scapin, A. Cheng, B. Q. Mercado, D. G. Waterman, T. Ganesh, S. Dallakyan, B. N. Read, T. Nieusma, K. W. Lucier, M. L. Mayer, N. J. Chiang, N. Poweleit, P. T. McGilvray, T. S. Wilson, M. Mashore, C. Hennessy, S. Thomson, B. Wang, C. S. Potter, B. Carragher, *Front. Mol. Biosci.* **2021**, *8*, https://doi.org/10.3389/fmolb.2021.648603.
[28] L. Palatinus, P. Brázda, P. Boullay, O. Perez, M. Klementová, S. Petit, V. Eigner, M. Zaarour, S. Mintova, *Science* **2017**, *355*, 166, https://doi.org/10.1126/science.aak9652.
[29] C. Jandl, G. Steinfeld, K. Li, P. K. C. Pang, C. L. Choi, C. Wang, P. Simoncic, I. D. Williams, *Symmetry* **2023**, *15*, 983, https://doi.org/10.3390/sym15050983.
[30] P. Brázda, L. Palatinus, M. Babor, *Science* **2019**, *364*, 667, https://doi.org/10.1126/science.aaw2560.
[31] B. Wang, Y. Lin, *Chem. Commun.* **2022**, *58*, 13071, https://doi.org/10.1039/D2CC05218K.
[32] D. P. Karothu, Z. Alhaddad, C. R. Göb, C. J. Schürmann, R. Bücker, P. Naumov, *Angew. Chem. Int. Ed.* **2023**, *62*, e202303761, https://doi.org/10.1002/anie.202303761.
[33] Y. Watanabe, S. Takahashi, S. Ito, T. Tokiwa, Y. Noguchi, H. Azami, H. Kojima, M. Higo, S. Ban, K. Nagai, T. Hirose, T. Sunazuka, T. Yaguchi, K. Nonaka, M. Iwatsuki, *Org. Biomol. Chem.* **2023**, *21*, 2320, https://doi.org/10.1039/D2OB02286A.
[34] K. Gurung, P. Šimek, A. Jegorov, L. Palatinus, *Acta Crystallogr., Sect. C:Struct. Chem.* **2024**, *80*, 56, https://doi.org/10.1107/S2053229624001359.
[35] H. Ahmed, A. Pöthig, K.-N. Truong, T. Bach, *Synlett* **2024**, *35*, 983, https://doi.org/10.1055/s-0042-1751527.
[36] I. B. Rietveld, F. Painsecq, C. Jandl, D. Stam, G. Coquerel, *Cryst. Growth Des.* **2024**, *24*, 5893, https://doi.org/10.1021/acs.cgd.4c00513.
[37] ELDIX Software Suite, Version 5.5.3; ELDICO Scientific AG: Allschwil, Switzerland, 2024
[38] Apex Suite of Crystallographic Software, APEX4, Version 2022.1-1; Bruker AXS Inc.: Madison, Wisconsin, USA, 2022.
[39] SAINT, Version 8.40B; Bruker AXS Inc.: Madison, Wisconsin, USA,2019.
[40] SADABS, Version 2016/2; Bruker AXS Inc.: Madison, Wisconsin, USA, 2016.
[41] G. M. Sheldrick, *Acta Crystallogr., Sect. D:Struct. Biol.* **2010**, *66*, 479, https://doi.org/10.1107/S0907444909038360.
[42] G. M. Sheldrick, *Acta Crystallogr., Sect. C:Struct. Chem.* **2015**, *71*, 3, https://doi.org/10.1107/S2053229614024218.
[43] C. B. Hübschle, G. M. Sheldrick, B. Dittrich, *J. Appl. Crystallogr.* **2011**, *44*, 1281, https://doi.org/10.1107/S0021889811043202.
[44] L.-M. Peng, *Micron* **1999**, *30*, 625, https://doi.org/10.1016/S0968-4328(99)00033-5.
[45] L. Palatinus, P. Brázda, M. Jelínek, J. Hrdá, G. Steciuk, M. Klementová, *Acta Crystallogr., Sect. B:Struct. Sci., Cryst. Eng. Mater.* **2019**, *75*, 512, https://doi.org/10.1107/S2052520619007534.
[46] V. Petříček, L. Palatinus, J. Plášil, M. Dušek, *Z. Kristallogr. Cryst. Mater.* **2023**, *238*, 271, https://doi.org/10.1515/zkri-2023-0005.